

are sought for structures with axisymmetric geometry but non-axisymmetric loads. The problem is therefore conveniently defined using cylindrical polar co-ordinates (axial z , radial r , circumferential θ), for which the general equations of equilibrium are well known (Love, 1944).

Harmonic decompositions along the tube axis and around the circumference will be used to simplify the analysis. Infinitely long structures are investigated here; the procedure described can, however, be used to study tubes where disturbances decay substantially before reaching the ends.

The solution being sought should be useful in examining the adequacy of shell theory and the assumptions on which shell theories are based (e.g. the Love–Kirchhoff assumptions for thin shell theory). Elastic stresses in laminated tubes could also be evaluated, and the response of thick cylinders with rib stiffeners and thick tubes deeply buried within an elastic medium could be estimated. Some of these applications will be briefly considered in this paper, while others will be left for subsequent studies.

Variations along the axis

Radial displacement u_r , circumferential displacement u_θ and axial displacement u_z , as well as normal stresses σ_{rr} , $\sigma_{\theta\theta}$, σ_{zz} and shear stresses $\sigma_{r\theta}$, $\sigma_{\theta z}$, σ_{zr} can be expressed as follows.

(a) For a single load pattern. Fourier transforms are employed

$$\begin{aligned}(u_r, u_\theta, w_z, v, \sigma_{rr}, \sigma_{\theta\theta}, \sigma_{zz}, \sigma_{r\theta}) &= 2 \int_0^\infty (U_r, U_\theta, W_z, V, S_{rr}, S_{\theta\theta}, S_{zz}, S_{r\theta}) \cos mz \, dm \\ (u_z, \sigma_{\theta z}, \sigma_{zr}) &= 2 \int_0^\infty (U_z, S_{\theta z}, S_{zr}) \sin mz \, dm\end{aligned}\quad (1)$$

where

$$\begin{aligned}(U_r, U_\theta, W_z, V, S_{rr}, S_{\theta\theta}, S_{zz}, S_{r\theta}) &= \frac{1}{\pi} \int_0^\infty (u_r, u_\theta, w_z, v, \sigma_{rr}, \sigma_{\theta\theta}, \sigma_{zz}, \sigma_{r\theta}) \cos mz \, dz \\ (U_z, S_{\theta z}, S_{zr}) &= \frac{1}{\pi} \int_0^\infty (u_z, \sigma_{\theta z}, \sigma_{zr}) \sin mz \, dz\end{aligned}\quad (2)$$

and

$$\begin{aligned}v &= \frac{\partial u_r}{\partial r} + \frac{u_r}{r} + \frac{1}{r} \frac{\partial u_\theta}{\partial \theta} + \frac{\partial u_z}{\partial z} \\ 2w_z &= \frac{u_\theta}{r} + \frac{\partial u_\theta}{\partial r} - \frac{1}{r} \frac{\partial u_r}{\partial \theta}.\end{aligned}\quad (3)$$

(b) For loading patterns which have period L in z . Fourier series expansions are used

$$\begin{aligned}(u_r, u_\theta, w_z, v, \sigma_{rr}, \sigma_{\theta\theta}, \sigma_{zz}, \sigma_{r\theta}) &= \sum_{m=0}^\infty (U_r, U_\theta, W_z, V, S_{rr}, S_{\theta\theta}, S_{zz}, S_{r\theta})_m \cos\left(\frac{2\pi mz}{L}\right) \\ (u_z, \sigma_{\theta z}, \sigma_{zr}) &= \sum_{m=0}^\infty (U_z, S_{\theta z}, S_{zr})_m \sin\left(\frac{2\pi mz}{L}\right)\end{aligned}\quad (4)$$

where for $\kappa_0 = 1$ and for $m > 0$, $\kappa_m = 2$

$$\begin{aligned}
 (U_r, U_\theta, W_z, V, S_{rr}, S_{\theta\theta}, S_{zz}, S_{r\theta})_m &= \frac{2\kappa_m}{L} \int_0^{L/2} (u_r, u_\theta, w_z, v, \sigma_{rr}, \sigma_{\theta\theta}, \sigma_{zz}, \sigma_{r\theta}) \cos\left(\frac{2\pi mz}{L}\right) dz \\
 (U_z, S_{\theta z}, S_{zr})_m &= \frac{2\kappa_m}{L} \int_0^{L/2} (u_z, \sigma_{\theta z}, \sigma_{zr}) \sin\left(\frac{2\pi mz}{L}\right) dx.
 \end{aligned} \tag{5}$$

While the response is assumed here to be symmetric about $z = 0$, non-symmetric problems can be examined using complex Fourier transforms or complete Fourier series.

Variations around the circumference

Use can also be made of Fourier series expansions in θ

$$\begin{aligned}
 (U_r, U_z, V, S_{rr}, S_{\theta\theta}, S_{zz}, S_{zr}) &= \sum_{n=0}^{\infty} (U_r, U_z, V, S_{rr}, S_{\theta\theta}, S_{zz}, S_{zr})^{(n)} \cos n\theta \\
 (U_\theta, W_z, S_{r\theta}, S_{\theta z}) &= \sum_{n=0}^{\infty} (U_\theta, W_z, S_{r\theta}, S_{\theta z})^{(n)} \sin n\theta
 \end{aligned} \tag{6}$$

where

$$\begin{aligned}
 (U_r, U_z, V, S_{rr}, S_{\theta\theta}, S_{zz}, S_{zr})^{(n)} &= \frac{\kappa_n}{\pi} \int_0^\pi (U_r, U_z, V, S_{rr}, S_{\theta\theta}, S_{zz}, S_{zr}) \cos n\theta \, d\theta \\
 (U_\theta, W_z, S_{r\theta}, S_{\theta z})^{(n)} &= \frac{\kappa_n}{\pi} \int_0^\pi (U_\theta, W_z, S_{r\theta}, S_{\theta z}) \sin n\theta \, d\theta.
 \end{aligned} \tag{7}$$

Harmonic equations

Use of eqn (6) with eqns (1) or (4) leads to equations of equilibrium:

$$\begin{aligned}
 \frac{\partial^2 V^{(n)}}{\partial r^2} + \frac{1}{r} \frac{\partial V^{(n)}}{\partial r} - \left(m^2 + \frac{n^2}{r^2}\right) V^{(n)} &= 0 \\
 \frac{\partial^2 W_z^{(n)}}{\partial r^2} + \frac{1}{r} \frac{\partial W_z^{(n)}}{\partial r} - \left(m^2 + \frac{n^2}{r^2}\right) W_z^{(n)} &= 0 \\
 \frac{\partial^2 U_z^{(n)}}{\partial r^2} + \frac{1}{r} \frac{\partial U_z^{(n)}}{\partial r} - \left(m^2 + \frac{n^2}{r^2}\right) U_z^{(n)} &= \frac{m(\lambda + G)}{G} V^{(n)}
 \end{aligned} \tag{8}$$

where

$$\begin{aligned}
 \lambda &= \frac{\nu E}{(1 + \nu)(1 - 2\nu)} \\
 G &= \frac{E}{2(1 + \nu)}.
 \end{aligned}$$

DISPLACEMENT FIELDS

Equations (8) have solutions:

$$\begin{aligned}
 V^{(n)} &= A_1 I_n(mr) + A_2 K_n(mr) \\
 W_z^{(n)} &= A_3 I_n(mr) + A_4 K_n(mr) \\
 U_z^{(n)} &= U_z^{(n)} - \frac{\lambda + G}{2Gm} r \frac{\partial V^{(n)}}{\partial r} = A_5 I_n(mr) + A_6 K_n(mr)
 \end{aligned} \tag{9}$$

where $U^{(n)}$ has been defined for convenience, A_1-A_6 are integration constants, and I_n and K_n are modified Bessel functions of the first and second kinds. Displacement fields are then

$$\begin{aligned} U_r^{(n)} &= \frac{(\lambda+2G)}{Gm^2} \frac{\partial V^{(n)}}{\partial r} - \frac{(\lambda+G)}{2Gm^2} \frac{\partial}{\partial r} \left(r \frac{\partial V^{(n)}}{\partial r} \right) - \frac{2n}{m^2} \frac{W_z^{(n)}}{r} - \frac{1}{m} \frac{\partial U^{(n)}}{\partial r} \\ U_\theta^{(n)} &= \frac{(\lambda+G)}{2Gm^2} n \frac{\partial V^{(n)}}{\partial r} - \frac{(\lambda+2G)}{Gm^2} n \frac{V^{(n)}}{r} + \frac{2}{m^2} \frac{\partial W_z^{(n)}}{\partial r} + \frac{n}{m} \frac{U^{(n)}}{r} \\ U_z^{(n)} &= \frac{(\lambda+G)}{2Gm} r \frac{\partial V^{(n)}}{\partial r} + U^{(n)}. \end{aligned} \quad (10)$$

STRESS FIELDS

Linear elastic constitutive relations (Love, 1944) can be used to find expressions for the stress fields :

$$\begin{aligned} S_{rr}^{(n)} &= (\lambda+2G)V^{(n)} - 2G \left(\frac{U_r^{(n)}}{r} + \frac{n}{r} U_\theta^{(n)} + m U_z^{(n)} \right) \\ S_{\theta\theta}^{(n)} &= \lambda V^{(n)} + 2G \left(\frac{U_r^{(n)}}{r} + \frac{n}{r} U_\theta^{(n)} \right) \\ S_{zz}^{(n)} &= \lambda V^{(n)} + 2Gm U_z^{(n)} \\ S_{r\theta}^{(n)} &= 2G \left(W_z^{(n)} - \frac{U_\theta^{(n)}}{r} - \frac{n}{r} U_r^{(n)} \right) \\ S_{\theta z}^{(n)} &= -G \left(\frac{n}{r} U_z^{(n)} + m U_\theta^{(n)} \right) \\ S_{zr}^{(n)} &= \frac{(\lambda+G)}{2m} \frac{\partial}{\partial r} \left(r \frac{\partial V^{(n)}}{\partial r} \right) - Gm U_r^{(n)}. \end{aligned} \quad (11)$$

STIFFNESS OF A THICK TUBE

Using eqns (9) with (10) and (11), displacement coefficients can be expressed as a function of the integration constants $\mathbf{A} = (A_1, A_2, A_3, A_4, A_5, A_6)^T$

$$(U_r^{(n)}, U_\theta^{(n)}, U_z^{(n)})^T = \mathbf{P}(r)\mathbf{A}. \quad (12)$$

Similar expressions can be found for the stress coefficients :

$$\begin{aligned} (S_{rr}^{(n)}, S_{\theta\theta}^{(n)}, S_{zr}^{(n)})^T &= \mathbf{Q}(r)\mathbf{A} \\ (S_{\theta\theta}^{(n)}, S_{zz}^{(n)}, S_{\theta z}^{(n)})^T &= \mathbf{R}(r)\mathbf{A}. \end{aligned} \quad (13)$$

The matrices \mathbf{P} , \mathbf{Q} and \mathbf{R} are given in the Appendix.

Stiffness equations for a long tube with internal radius a and external radius b are then

$$\mathbf{KD} = \mathbf{F} \quad (14)$$

where the displacements and tractions at internal and external boundaries are :

$$\begin{aligned} \mathbf{D} &= (U_r(a), U_\theta(a), U_z(a), U_r(b), U_\theta(b), U_z(b))^T \\ \mathbf{F} &= (aS_{rr}(a), aS_{r\theta}(a), aS_{zr}(a), -bS_{rr}(b), -bS_{r\theta}(b), -bS_{zr}(b))^T \end{aligned} \quad (15)$$

and the symmetric stiffness matrix is given by

$$\mathbf{K} = \begin{pmatrix} a\mathbf{Q}(a) \\ -b\mathbf{Q}(b) \end{pmatrix} \begin{pmatrix} \mathbf{P}(a) \\ \mathbf{P}(b) \end{pmatrix}^{-1}. \quad (16)$$

SOLUTION PROCEDURE

The harmonic tube response to a particular set of applied loads is found as follows.

- Boundary tractions σ_{rr} , $\sigma_{\theta z}$, σ_{zr} are integrated [eqns (7) with (2) or (5)] to determine each harmonic term.
- Harmonic stiffness equations are assembled, and then the solution for harmonic boundary displacement is evaluated.
- Integration constants \mathbf{A} are evaluated from:

$$\mathbf{A} = \begin{pmatrix} \mathbf{P}(a) \\ \mathbf{P}(b) \end{pmatrix}^{-1} [U_r^{(n)}(a), U_\theta^{(n)}(a), U_z^{(n)}(a), U_r^{(n)}(b), U_\theta^{(n)}(b), U_z^{(n)}(b)]^T. \quad (17)$$

- Equations (12) and (13) are used to determine displacements or stresses at any radial position r .

The harmonic response needs to be summed according to eqns (6) and (4) or (1). Naturally, Fourier Series summations are evaluated up to a finite value of m or n . Gaussian quadrature has been used to invert the Fourier transforms.

LAMINATED STRUCTURES

It is straightforward to determine the response of long tubular structures composed of a series of interlocking tubes, by combining tube stiffness equations using conventional matrix assembly techniques (Zienkiewicz, 1971). The interfaces are assumed to be perfectly bonded together, so that there is full compatibility of displacements and full transfer of shear stresses $\sigma_{\theta z}$, σ_{zr} and normal stress σ_{rr} between one tube and the next. Displacements and stresses within any particular tube are found by using eqn (17) with the internal and external boundary displacements for that particular laminate.

EXAMPLE CALCULATIONS

Four example problems are now briefly considered in order to demonstrate the solution.

Thin tube response to ring load

Figure 2 shows estimates of radial displacement w along a long tube with midsurface radius a , thickness $h = a/10$, modulus E and Poisson's ratio $\nu = 0.25$, loaded with a single band of radial pressure p (band width $2d$). Timoshenko and Woinowsky-Krieger (1959) examined the response of a long cylindrical shell subjected to a line load P (equivalent to $2dp$) around the circumference. That solution is shown, as well as thick tube solutions for pressure bands with $a/d = 5$ and 2. A thin shell solution for pressure band $a/d = 5$ is also given; the shell theory solution of Herrmann and Armenakas (1962) is summarized in the Appendix. Booker and Carter (1984) give details of the harmonic components of transformed traction, used to determine these pressure band solutions.

There is close agreement between the closed form solution of Timoshenko and the pressure band solutions for $a/d = 5$. For a tube of this thickness, the shell theory appears to be a very satisfactory approximation. Widening the pressure band to $a/d = 2$ reduces

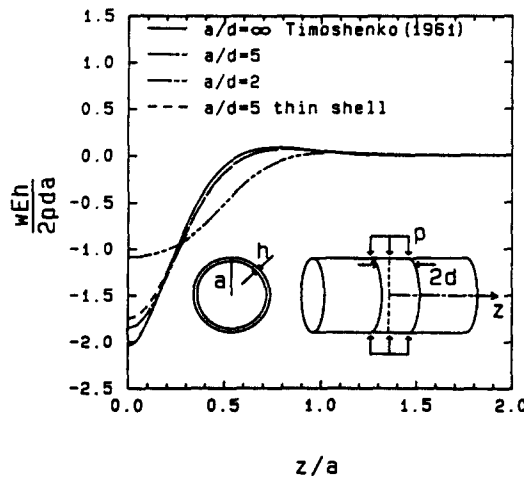


Fig. 2. Response of a thin cylinder to a band of radial pressure ($\nu = 0.25, h = a/10$).

the maximum radial deflection and extends the deformations along the structure. These comparisons could, for example, be extended to include a study of displacement and stress distributions across the tube thickness. [See Moore (1988) for a study of this type for dynamic tube response.]

Thick tube response to patch load

The response of a thick tube (midsurface radius a , thickness $h = a$, Poisson's ratio 0.25) is illustrated in Fig. 3. A double patch load is applied to the structure with angular width 2δ and length along the axis $2d$. The radial response along the structure is shown for $\delta = 90^\circ$ (the axisymmetric case), $\delta = 45^\circ$ and $\delta = 22.5^\circ$.

The solution can also be used to determine the response to patch load of the internal boundary of a very thick tube (external boundary remote). The solutions thus generated match those of Booker and Carter (1984).

Laminated pipe response to periodic ring load

The last example problems to be examined, feature a tube composed of two laminates. An interface radius at $r = a$ connects an inner tube of modulus E_i , Poisson's ratio $\nu_i = 0.35$, and an outer tube of modulus $E_o = 3E_i$ and Poisson's ratio $\nu_o = 0.25$. Both laminates have thickness $a/10$, so that total thickness $h = a/5$. The response of the system is determined for a series of pressure bands of width $2d = a/5$ and spacing L .

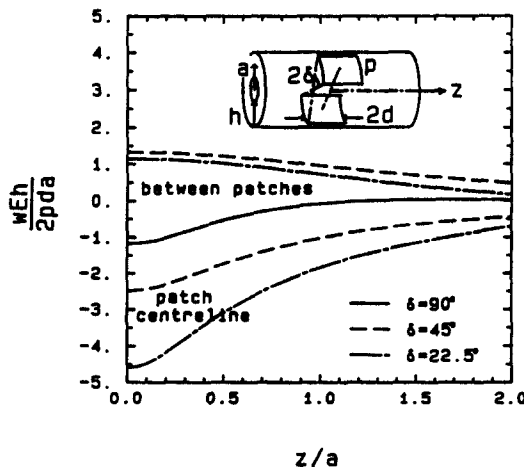


Fig. 3. Radial response along a thick tube loaded with patch loads ($d/a = 0.2, \nu = 0.25, h = a$).

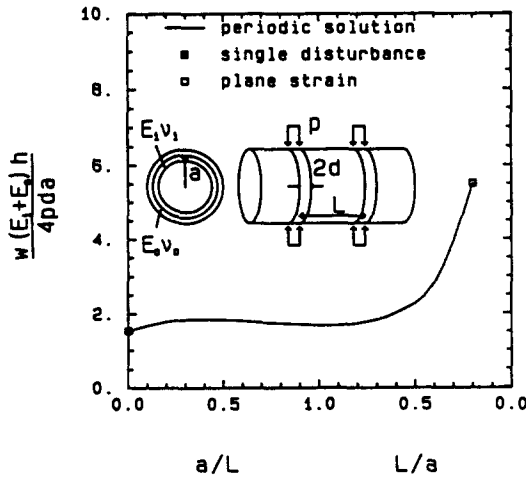


Fig. 4. Peak radial response of a laminated tube subjected to periodic ring loads ($d/a = 0.1, h = a/5, \nu_1 = 0.35, \nu_0 = 0.25, E_0 = 3E_1$).

Figure 4 shows predictions of peak radial deformation along the interface, evaluated for various band spacings L . At $a/L = 0$, the band is effectively isolated from all the others and the single disturbance solution based on Fourier transforms has been employed. At $L/a = 0.2$ the bands link up, and the plane strain solution is generated. Both of these special solutions are indicated.

The interaction stresses may be of significance for a laminated structure. Figure 5 shows predictions of maximum normal stress σ_{rr} and shear stress σ_{rz} between the tube laminates. Solutions are again shown for a range of pressure band spacings. Maximum normal stress occurs under the midpoint of the loaded region, and it is not greatly affected by band spacing L . Generally, maximum shear stress occurs just beyond the edge of the loaded zone. Greatest shear stress occurs when pressure band spacings are about equal to the tube radius. Naturally shear stress is zero for the plane strain condition.

Response of laminated pipe with rib stiffeners

One situation where the pipe may be subjected to loads similar to those considered in the last section, is that of a pipe fitted with regularly spaced rib stiffeners. If the stiffened pipe is placed in a fluid (or if it is filled with a fluid) the response can be subdivided into two components. Firstly, the external fluid pressure pressing on an unstiffened tube generates a uniform contraction w_{ps} , which takes place under plane strain conditions. Secondly there

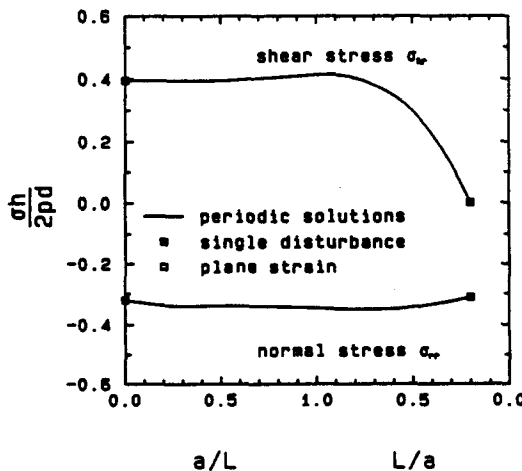


Fig. 5. Peak normal and shear stresses acting between laminates of tube under periodic ring load.

are bands of radial pressure associated with each rib stiffener, which lead to outward deformations w_0 wherever stiffeners are located.

Figure 4 can be used to estimate the ring thrust which develops in a stiffener attached to this particular laminated pipe. The dependent variable denoted by

$$I = \frac{w(E_i + E_0)h}{4pda}$$

is a function of a/L . Using the plane strain solution I_{ps} (for $L/a = 0.2$) marked on Fig. 4, and using q to denote the external fluid pressure, the plane strain displacement is

$$w_{ps} = \frac{2I_{ps}qa}{(E_i + E_0)}.$$

A stiffener which permits no radial movement will ensure that

$$w_0 = \frac{4Ipda}{h(E_i + E_0)} = w_{ps}$$

so that the force acting radially around the internal stiffener surface is

$$2pd = \frac{I_{ps}qh}{I}$$

and the hoop thrust generated in the stiffener is

$$2pda = \frac{I_{ps}qha}{I}.$$

The same approach can be used to estimate from Fig. 4 the maximum shear and normal stresses acting across the interface of the laminated stiffened pipe.

CONCLUSIONS

An exact solution for evaluating the three-dimensional response of long thick elastic tubes has been described. The harmonic response is evaluated, and summations are undertaken and Fourier transforms are inverted in order to evaluate structural response to non-harmonic loading systems. The solution has been used to solve a number of problems involving long elastic tubes. The procedure should also prove useful in validating other methods of analysis (e.g. three-dimensional finite element analysis).

REFERENCES

- Booker, J. R. and Carter, J. P. (1984). Analysis of deformation caused by loadings applied to the walls of a circular tunnel. *Int. J. Numer. Analyt. Meth. Geomech.* **8**(5), 445–455.
- Flügge, W. (1960). *Stresses in Shells*. Springer, Berlin.
- Herrmann, G. and Armenakas, A. E. (1962). Dynamic behaviour of cylindrical shells under initial stress. *Proc. Fourth Natl. Cong. Applied Mechanics, ASME* **1**, 203–213.
- Love, A. E. H. (1944). *A Treatise on the Mathematical Theory of Elasticity*, Fourth Edn. Dover, New York.
- Moore, I. D. (1988). *Vibration of Thick Elastic and Viscoelastic Tubes—Harmonic Response*. Department of Civil Engineering and Surveying, University of Newcastle, Research Report No. 035.11.1988. ISBN 0 7259 0638 3. University of Newcastle, Newcastle.
- Mushkhelishvili, N. I. (1972). *Rock Mechanics and the Mathematical Theory of Elasticity*. P. Noordhoff, Groningen, The Netherlands.
- Timoshenko, S. P. and Woinowsky-Krieger, S. (1959). *Theory of Plates and Shells*. McGraw-Hill, New York.
- Zienkiewicz, O. C. (1971). *The Finite Element Method in Engineering Science*. McGraw-Hill, London.

APPENDIX

Displacement and stress fields for a thick tube

Displacement coefficients in the radial, circumferential and axial directions are given by :

$$\begin{pmatrix} U_r^{(n)} \\ U_\theta^{(n)} \\ U_z^{(n)} \end{pmatrix} = \mathbf{P}(r)\mathbf{A} = \begin{pmatrix} \mathbf{P}_1 \\ \mathbf{P}_2 \\ \mathbf{P}_3 \end{pmatrix} \mathbf{A}$$

where \mathbf{A} is the vector of integration constants.

$$\mathbf{P}(r) = \begin{pmatrix} C_2 I' - C_1(I' + I''r)/2 & C_2 K' - C_1(K' + K''r)/2 & \frac{-2nI}{rm^2} & \frac{-2nK}{rm^2} & \frac{-I'}{m} & \frac{-K'}{m} \\ nC_1 I'/2 - nC_2 I/r & nC_1 K'/2 - nC_2 K/r & \frac{2I'}{m^2} & \frac{2K'}{m^2} & \frac{nI}{rm} & \frac{nK}{rm} \\ \frac{mC_1 r I'}{2} & \frac{mC_1 r K'}{2} & 0 & 0 & I & K \end{pmatrix}$$

and

$$C_1 = \frac{\lambda + G}{Gm^2}$$

$$C_2 = \frac{\lambda + 2G}{Gm^2}$$

with

$$I = I_n(mr), \quad I' = \frac{d}{dr}(I_n(mr)), \quad I'' = \frac{d^2}{dr^2}(I_n(mr))$$

$$K = K_n(mr), \quad K' = \frac{d}{dr}(K_n(mr)), \quad K'' = \frac{d^2}{dr^2}(K_n(mr)).$$

Stress coefficients S_{rr} , $S_{\theta\theta}$, S_{zz} are given by :

$$\begin{pmatrix} S_{rr} \\ S_{\theta\theta} \\ S_{zz} \end{pmatrix} = \mathbf{Q}(r)\mathbf{A}$$

where

$$\mathbf{Q}(r) = \begin{pmatrix} (\lambda + 2G)I & (\lambda + 2G)K & 0 & 0 & 0 & 0 \\ 0 & 0 & 2GI & 2GK & 0 & 0 \\ \frac{GmC_1(I' + rI'')}{2} & \frac{GmC_1(K' + rK'')}{2} & 0 & 0 & GI' & GK' \end{pmatrix} - 2G \begin{pmatrix} P_1/r + nP_2/r + mP_3 \\ P_2/r + nP_1/r \\ -mP_1/2 \end{pmatrix}$$

Coefficients $S_{\theta\theta}$, S_{zz} and $S_{\theta z}$ are:

$$\begin{pmatrix} S_{\theta\theta} \\ S_{zz} \\ S_{\theta z} \end{pmatrix} = \mathbf{R}(r)\mathbf{A}$$

where

$$\mathbf{R}(r) = \begin{pmatrix} \lambda I & \lambda K & 0 & 0 & 0 & 0 \\ \lambda I & \lambda K & 0 & 0 & 0 & 0 \\ 0 & 0 & 0 & 0 & 0 & 0 \end{pmatrix} + 2G \begin{pmatrix} P_1/r + nP_2/r \\ mP_3 \\ nP_3/r + mP_2 \end{pmatrix}$$

Stiffness equations for a shell

The shell theory of Herrmann and Armenakas (1962) yields the following equations relating displacement coefficients to boundary tractions for a shell of thickness h with midsurface radius r

$$r \begin{pmatrix} S_{rr}^{(n)} \\ S_{\theta\theta}^{(n)} \\ S_{zr}^{(n)} \end{pmatrix} = (K_{ij}) \begin{pmatrix} U_r^{(n)} \\ U_{,\theta}^{(n)} \\ U_{,z}^{(n)} \end{pmatrix}$$

where

$$K_{11} = -\frac{E_p}{r} - \frac{D(n^2-1)^2}{r^3} - rDm^3 - \frac{2Dm^2n^2}{r}$$

$$K_{12} = K_{21} = -\frac{E_p n}{r} - \frac{D(3-\nu)m^2n}{2r}$$

$$K_{13} = K_{31} = -\nu E_p m - Dm^3 + \frac{G_p h^2 n^2 m}{12r^2}$$

$$K_{22} = -\frac{E_p n^2}{r} - G_p \left(1 + \frac{h^2}{4r^2}\right) m^2 r$$

$$K_{23} = K_{32} = -nmE_p(1+\nu)/2$$

$$K_{33} = -m^2 E_p r - n^2 \frac{G_p}{r} \left(1 + \frac{h^2}{12r^2}\right)$$

for modulus E , Poisson's ratio ν and

$$E_p = \frac{Eh}{1-\nu^2}$$

$$D = \frac{Eh^3}{12(1-\nu^2)}$$

$$G_p = \frac{Eh}{2(1+\nu)}$$